International Journal of Biological Macromolecules 70 (2014) 131–137

Contents lists available at ScienceDirect

International Journal of Biological Macromolecules

journal homepage: www.elsevier.com/locate/ijbiomac

Quantitative analysis of histamine- and agmatine–DNA interactions using surface plasmon resonance

Carla Cruz*[,1], Ângela Sousa[1], Élia Mota, Fani Sousa, João A. Queiroz

CICS-UBI – Centro de Investigação em Ciências da Saúde, Universidade da Beira Interior, Av. Infante D. Henrique, 6200-506 Covilhã, Portugal

ARTICLE INFO

Article history:
Received 30 January 2014
Received in revised form 23 June 2014
Accepted 24 June 2014
Available online 30 June 2014

Keywords:
Surface plasmon resonance
Affinity ligands
Plasmid DNA

ABSTRACT

To exploit the binding affinity for efficient plasmid purification, agmatine and histamine were immobilized on carboxymethylated dextran surface. Their binding strength is evaluated with oligonucleotides and pUC19 (2.69 kbp), pVAX1-*LacZ* (6.05 kbp) and pcDNA3-myc-FLNa S2152A (14 kbp) isoforms by measuring the K_D using SPR-biosensor. The oligonucleotides and plasmid isoforms bind more strongly to histamine than to agmatine. Concerning the oligonucleotides, the highest affinities are found for poly 30, and polyT and polyG series showed lowest affinity with both ligands. These results are corroborating with the hetero-oligonucleotides since the lowest binding affinity is found for GGGTTT, indicating that thymidine and guanosine together decrease the binding strength. The largest plasmid has the highest binding, while pUC19 shows the weaker binding. The linear isoform exhibit the highest binding affinity to both amino acid-derivatives.

Decreasing the pH above 6, the interaction strength of linear isoform increases possibly due to positively charged of the surface, which enhances electrostatic interactions. However, no binding response is detected with high salt concentrations (1 M NaCl) and for different buffers. The affinity information accessible with the biosensor offers new insight into nucleic acids–ligand interactions, as well as, new criteria leading the optimization of the novel ligands for preparative plasmid purification.

1. Introduction

The characterization of amino acid–DNA interactions is important for regulating many cellular processes, including DNA transcription, replication and repair [1,2]. Fewer methods are available to measure amino acid–DNA interaction affinities, such as, fluorescence, nuclear magnetic resonance (NMR), isothermal titration calorimetry (ITC) or surface plasmon resonance (SPR) [3,4]. Calorimetry and NMR are normally limited by their sensitivity, whereas fluorescence typically requires either the amino acid or the DNA to be labelled with a fluorophore [5,6]. On the other hand, SPR-biosensor can be used with low sample quantities and is able to measure binding constants and on and off rates across a very wide range of concentrations [7,8].

Agmatine and histamine, derivatives of amino acids L-arginine and L-histidine, containing basic guanidinium group and imidazole ring on a spacer arm, respectively, have been reported as polyamines binders of calf-thymus DNA [9,10]. In light of biofunctions of agmatine and the cell penetrating ability of its guanidine, it was used to synthetize a gene vector for DNA *in vitro* and *in vivo* delivery [11]. Recently, histamine has also been reported in affinity chromatography as a multimodal ligand for the separation of pDNA isoforms under different chromatographic conditions [12]. To the best of our knowledge, there is no study on agmatine and histamine recognition with oligonucleotides and pDNA that focuses the nucleotides binding preferences and explores the interactions that govern the efficiency of these ligands in pDNA isoforms separation.

Here we employ SPR-biosensor to quantify the strength of binding for the affinity process between agmatine and histamine (acting as affinity ligands) and oligonucleotides or different isoforms of pUC19, pVAX1-*LacZ* and pcDNA3-myc-FLNa S2152A plasmids. The agmatine and histamine were immobilized on sensor chip surface to mimic immobilized ligands in affinity chromatographic support (see Fig. 1). The effect of buffers composition and pH in the binding of linearpVAX1-*LacZ* isoform was evaluated.

The experimental data allowed us to get binding information to improve plasmid purification with low sample consumption, rapid and automated analysis by using histamine and agmatine as ligands in affinity chromatography.

* Corresponding author. Tel.: +351 275 329 097; fax: +351 275 329 099.
E-mail address: carlacruz@fcsaude.ubi.pt (C. Cruz).
[1] These authors contributed equally to this work.

http://dx.doi.org/10.1016/j.ijbiomac.2014.06.044
0141-8130/

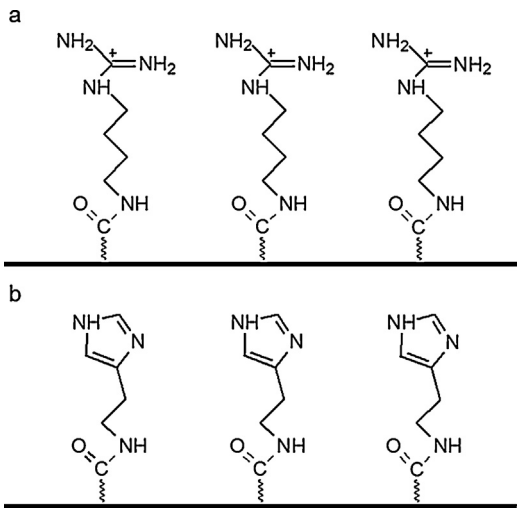

Fig. 1. Schematic structures of (a) agmatine and (b) histamine immobilized on surface of activated carboxymethyldextran.

2. Materials and methods

The 2.69-kbp pUC19 plasmid and 6.05-kbp pVAX1-*LacZ* plasmid with ampicillin and kanamycin resistance respectively, were provided by Invitrogen (Carlsband, CA, USA). The 14-kbp pcDNA3-myc-FLNa S2152A, Addgene plasmid 8983, (pcDNA3-based plasmid) [13] with both ampicillin and neomycin resistance was acquired from Addgene (Cambridge, USA). The restriction enzymes Sma I and Hind III were from Takara (Otsu, Shiga, Japan) and the molecular weight marker HyperLadderTM I was from Bioline (Taunton, MA, USA). The GreenSafe Premium was purchased to NZYTech (Lisbon, Portugal).

2.1. Bacterial growth conditions to obtain pUC19, pVAX1-LacZ and pcDNA3-myc-FLNa S2152A plasmids

The three plasmids amplification was performed by autonomous replication in *Escherichia coli* (*E. coli*) DH5α host. The cell growth was carried out at 37 °C overnight in a shake flask with 250 mL of Terrific Broth medium (20 g/L tryptone, 24 g/L yeast extract, 4 mL/L glycerol, 0.017 M KH_2PO_4, 0.072 M K_2HPO_4) supplemented with 100 μg/mL ampicillin for pUC19, 30 μg/mL kanamycin for pVAX1-*LacZ* and 100 μg/mL ampicillin

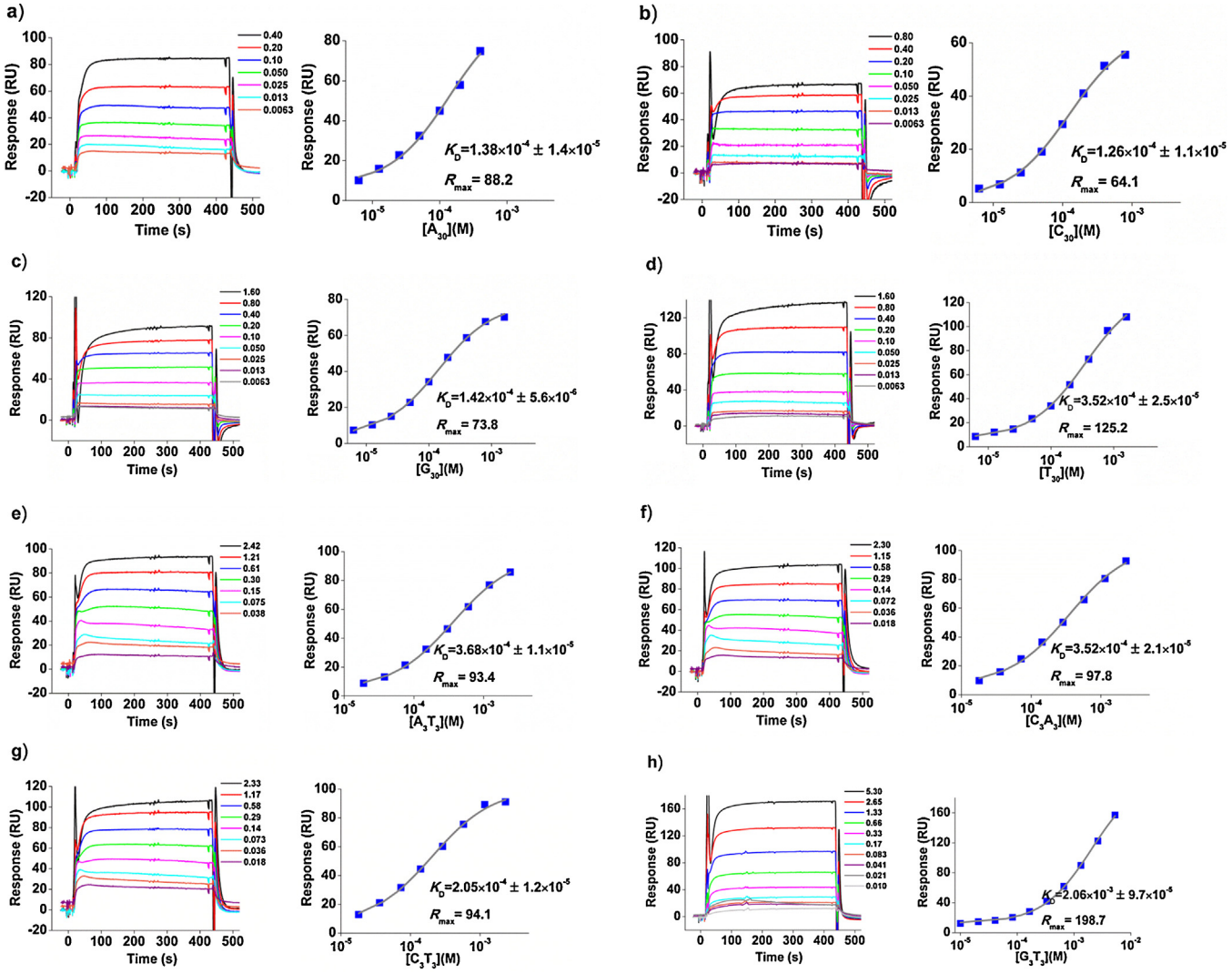

Fig. 2. Sensorgrams and equilibrium-binding analysis of immobilized histamine to (a) polyA$_{30}$, (b) polyC$_{30}$, (c) polyG$_{30}$, (d) polyT$_{30}$, (e) polyA$_3$T$_3$, (f) polyC$_3$A$_3$, (g) polyC$_3$T$_3$ and (h) polyG$_3$T$_3$ in 10 mM Tris–HCl pH 8.

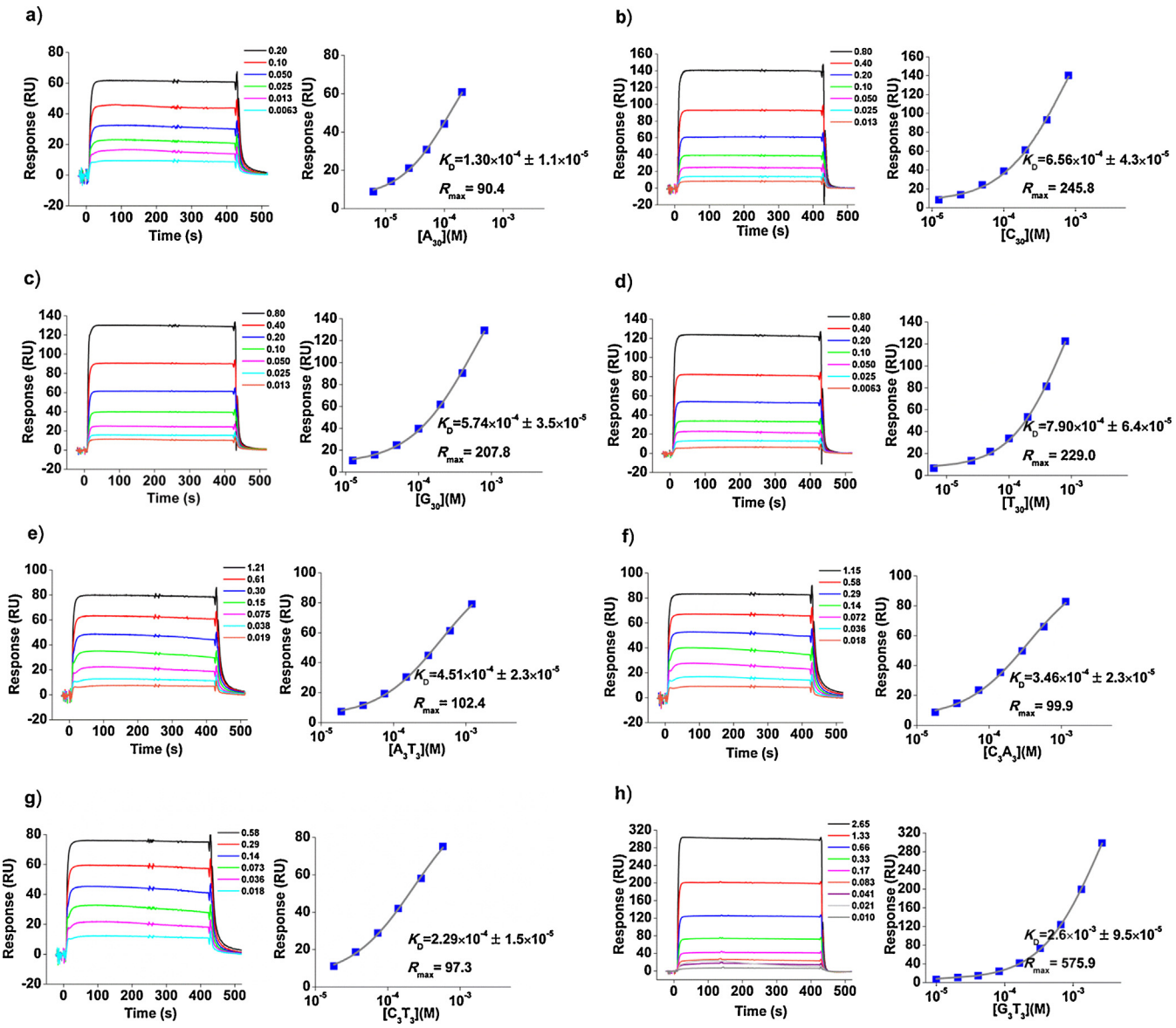

Fig. 3. Sensorgrams and equilibrium-binding analysis of immobilized agmatine to (a) polyA$_{30}$, (b) polyC$_{30}$, (c) polyG$_{30}$, (d) polyT$_{30}$, (e) polyA$_3$T$_3$, (f) polyC$_3$A$_3$, (g) polyC$_3$T$_3$ and (h) polyG3T3in 10 mM Tris–HCl pH 8.

plus 25 μg/mL neomycin for pcDNA3-based plasmid. Each desired plasmid was constructed with resistance genes to specific antibiotics, which are used as selection markers for the exclusive growth of transformed cells. The fermentation was carried out overnight, at 37 °C under 250 rpm shaking. Bacterial cell growth was monitored by measuring the OD_{600} using a Pharmacia Biotech Ultraspec 3000 (Cambridge, England) and suspended at late log phase ($OD_{600} \approx 10$). The cells were recovered by centrifugation and stored at −20 °C.

2.2. Alkaline lysis and primary isolation of pUC19, pVAX1-LacZ and pcDNA3-myc-FLNa S2152A plasmid isoforms

The pUC19, pVAX1-*LacZ* and pcDNA3-myc-FLNa S2152A were recovered from *E. coli* bacteria by using the NZYTech (Lisbon, Portugal) plasmid Maxiprep kit according to the manufacturer's instructions. This protocol is based on a modified alkaline lysis procedure. Following lysis, the plasmid DNA was pre-purified in NZYTech columns charged with a silica-based anion-exchange resin. After, the pDNA was eluted from the columns and concentrated through an isopropanol precipitation. The resultant pellet was dissolved in 10 mM Tris–HCl buffer (pH 8.0) where the supercoiled (sc) plasmid isoform is the most predominant (around 99%). Pure samples of open circular (oc) and linear plasmid isoforms were prepared from previous sc-enriched plasmid sample. In this way, oc plasmid samples were prepared by incubating scpDNA samples at room temperature (24 °C). The samples were monitored over the time by electrophoretic analysis until the total conversion of sc plasmid to oc isoform was observed (about 3 days). On the other hand, linear plasmid samples were prepared by enzymatic digestion of the pUC19 plasmid with the Sma I enzyme and the pVAX1-*LacZ* and pcDNA3-myc-FLNa S2152A plasmids with the Hind III enzyme, during 1 h of incubation at 37 °C.

2.3. Agarose gel electrophoresis

The homogeneity and content of plasmid isoforms present in each prepared sample was analyzed by horizontal electrophoresis using 15 cm, 0.8% agarose (Hoefer, San Francisco, CA, USA) gels, stained with GreenSafe Premium (1 μg/mL). Electrophoresis was

Table 1
Equilibrium analysis of the oligonucleotides/plasmids in 10 mM of Tris–HCl pH 8.

Nucleotides/plasmids	Agmatine K_D[a] (M) ± SD[b]	Histamine K_D[a] (M) ± SD[b]
5′-AMP	$9.33 \times 10^{-3} \pm 3.6 \times 10^{-4}$	$3.99 \times 10^{-3} \pm 1.4 \times 10^{-4}$
A3	$1.50 \times 10^{-3} \pm 6.7 \times 10^{-5}$	$8.11 \times 10^{-4} \pm 5.0 \times 10^{-5}$
A6	$1.58 \times 10^{-4} \pm 1.7 \times 10^{-5}$	$1.60 \times 10^{-4} \pm 2.7 \times 10^{-5}$
A15	$1.45 \times 10^{-4} \pm 1.2 \times 10^{-5}$	$1.34 \times 10^{-4} \pm 1.2 \times 10^{-5}$
A30	$1.30 \times 10^{-4} \pm 1.1 \times 10^{-5}$	$1.38 \times 10^{-4} \pm 1.4 \times 10^{-5}$
C3	$1.48 \times 10^{-3} \pm 5.0 \times 10^{-5}$	$1.03 \times 10^{-3} \pm 4.7 \times 10^{-5}$
C6	$1.10 \times 10^{-3} \pm 9.7 \times 10^{-5}$	$4.40 \times 10^{-4} \pm 2.9 \times 10^{-5}$
C15	$1.80 \times 10^{-3} \pm 1.1 \times 10^{-4}$	$3.09 \times 10^{-4} \pm 1.8 \times 10^{-5}$
C30	$6.56 \times 10^{-4} \pm 4.3 \times 10^{-5}$	$1.26 \times 10^{-4} \pm 1.1 \times 10^{-5}$
5′-GMP	$1.02 \times 10^{-2} \pm 5.1 \times 10^{-4}$	$3.29 \times 10^{-3} \pm 2.0 \times 10^{-4}$
G3	$1.39 \times 10^{-3} \pm 2.0 \times 10^{-4}$	$1.52 \times 10^{-3} \pm 5.0 \times 10^{-4}$
G6	$3.39 \times 10^{-3} \pm 7.5 \times 10^{-4}$	$6.64 \times 10^{-4} \pm 5.9 \times 10^{-5}$
G15	$3.73 \times 10^{-4} \pm 4.3 \times 10^{-5}$	$3.70 \times 10^{-4} \pm 4.2 \times 10^{-5}$
G30	$5.74 \times 10^{-4} \pm 3.5 \times 10^{-5}$	$1.42 \times 10^{-4} \pm 5.6 \times 10^{-6}$
5′-TMP	$8.45 \times 10^{-3} \pm 5.6 \times 10^{-4}$	$4.06 \times 10^{-3} \pm 3.8 \times 10^{-4}$
T3	$2.48 \times 10^{-3} \pm 2.3 \times 10^{-4}$	$2.01 \times 10^{-3} \pm 3.0 \times 10^{-4}$
T6	$7.78 \times 10^{-4} \pm 7.7 \times 10^{-5}$	$5.32 \times 10^{-4} \pm 3.7 \times 10^{-5}$
T15	$1.56 \times 10^{-3} \pm 1.3 \times 10^{-4}$	$4.98 \times 10^{-4} \pm 2.7 \times 10^{-5}$
T30	$7.90 \times 10^{-4} \pm 6.4 \times 10^{-5}$	$3.52 \times 10^{-4} \pm 2.5 \times 10^{-5}$
A3T3	$4.51 \times 10^{-4} \pm 2.3 \times 10^{-5}$	$3.68 \times 10^{-4} \pm 1.1 \times 10^{-5}$
C3A3	$3.46 \times 10^{-4} \pm 2.3 \times 10^{-5}$	$3.52 \times 10^{-4} \pm 2.1 \times 10^{-5}$
C3T3	$2.29 \times 10^{-4} \pm 1.5 \times 10^{-5}$	$2.05 \times 10^{-4} \pm 1.2 \times 10^{-5}$
G3T3	$2.58 \times 10^{-3} \pm 9.5 \times 10^{-5}$	$2.06 \times 10^{-3} \pm 9.7 \times 10^{-5}$
sc pUC19	$2.97 \times 10^{-8} \pm 2.1 \times 10^{-9}$	$2.41 \times 10^{-8} \pm 4.0 \times 10^{-9}$
oc pUC19	$5.51 \times 10^{-9} \pm 8.8 \times 10^{-10}$	$6.37 \times 10^{-9} \pm 1.2 \times 10^{-9}$
ln pUC19	$1.07 \times 10^{-9} \pm 8.3 \times 10^{-11}$	$1.03 \times 10^{-9} \pm 1.0 \times 10^{-10}$
sc pVAX1-*LacZ*	$1.97 \times 10^{-7} \pm 8.6 \times 10^{-9}$	$1.20 \times 10^{-7} \pm 8.4 \times 10^{-9}$
oc pVAX1-*LacZ*	$1.29 \times 10^{-9} \pm 9.3 \times 10^{-11}$	$1.33 \times 10^{-9} \pm 1.4 \times 10^{-10}$
ln pVAX1-*LacZ*	$7.73 \times 10^{-10} \pm 2.1 \times 10^{-11}$	$6.27 \times 10^{-10} \pm 3.7 \times 10^{-11}$
scpcDNA-Myc-FLNA	$5.33 \times 10^{-8} \pm 3.8 \times 10^{-9}$	$3.47 \times 10^{-8} \pm 4.8 \times 10^{-9}$
ocpcDNA-Myc-FLNA	$3.10 \times 10^{-8} \pm 1.4 \times 10^{-9}$	$1.05 \times 10^{-8} \pm 2.0 \times 10^{-9}$
lnpcDNA-Myc-FLNA	$1.63 \times 10^{-10} \pm 2.4 \times 10^{-11}$	$1.75 \times 10^{-10} \pm 1.8 \times 10^{-11}$

[a] Equilibrium dissociation constant.
[b] Standard deviation.

carried out at 100 V, for 40 min, with TAE buffer (40 mM Tris base, 20 mM acetic acid and 1 mM EDTA, pH 8.0)

2.4. SPR measurements

All SPR experiments were performed on a Biacore T200 system using carboxymethyl dextran sensor chip CM5. The carboxylic groups on the surface were activated for 7 min using a mixture of 0.4 M 1-ethyl-3-(3-dimethylaminopropyl) carbodiimide (EDC) and 0.1 M N-hydroxysuccinimide (NHS) to create reactive succinimide esters, followed by a brief washing step with HBS-N. Agmatine and histamine were then injected at pH 8.5, dissolved in 0.1 M borate solution in running buffer of 10 mM HBS-N. Finally, unreacted esters are blocked with 1 M of ethanolamine.

Flow cell 2 contained 159 RU of agmatine and flow cell 3 contained 156 RU of histamine. Flow cell 1 was left blank to be used as a reference surface.

In the experiments flow cell 1 act as a control reference and is used to correct the bulk refractive index changes and non-specific binding at the sensor surfaces. The sensorgram of the control cell is subtracted from the sensorgram of the cell of interest and data analysis is then performed on the control-corrected sensorgram. The modified surfaces were equilibrated with 10 mM Tris–HCl pH 8 as the running buffer in affinity measurements.

The oligonucleotides and plasmids were injected over the surfaces at least two repeats. The concentrations injected for oligonucleotides range between 5.3 mM and 6.3 μM and for plasmids isoforms between 12.5 μM and 0.012 nM. No regeneration

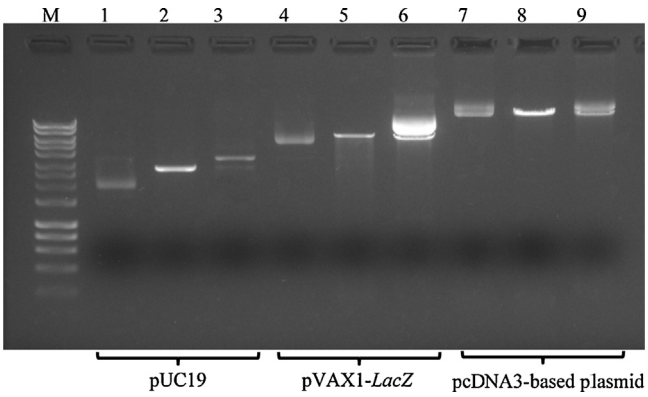

Fig. 4. Agarose gel electrophoretic analysis of plasmid samples prepared with different isoforms. Lane M: molecular weight marker; Lane 1, 2 and 3: pUC19 plasmid samples mainly containing sc, linear and oc isoforms, respectively; Lane 4, 5 and 6: pVAX1-*LacZ* plasmid samples containing sc, linear and oc isoforms, respectively; Lane 7, 8 and 9: pcDNA3-based plasmid samples containing sc, linear and oc isoforms, respectively.

solution was required since the analytes were removed from the sensor surfaces. Signals were automatically corrected using the control flow cell without immobilized amino acid and at least two repeats of each experiment were carried out. Steady state binding analysis was performed with multiple injections of different analytes concentrations over the immobilized surfaces for a 7 min period at flow rate 2 μL/min at 25 °C. The multiple sensorgrams from different concentrations of analyte were overlaid and aligned. The response in a steady state region is proportional to the amount of bound analyte and was determined by linear averaging over a 50 s timespan. To obtain the affinity constants, the results from the steady state region were fitted using a non-linear least square optimization of the binding parameters available within BIAevaluation software.

3. Results and discussion

Agmatine and histamine were tested for their ability to interact with oligonucleotides and pUC19, pVAX1-*LacZ* and pcDNA3-myc-FLNa S2152Aplasmidisoforms (supercoiled, opencircular and linear). For this purpose, agmatine and histamine were immobilized on CM5 sensor chip *via* amine coupling through its α-NH_2 groups. Sensorgrams regarding the oligonucleotides binding to histamine and agmatine are presented in Figs. 2 and 3, respectively. The K_D values are listed in Table 1. These examples show that affinity values (K_D) could be determined for all analytes, but not the rate constants due to very fast kinetics as in previous works [14,15]. In general, all oligonucleotides bind more strongly to histamine than agmatine surface in the conditions used. Values for the equilibrium dissociation constants ranged from 1.26×10^{-4} to 4.10×10^{-3} M for histamine and from 1.30×10^{-4} to 1.10×10^{-2}M for agmatine, both indicate low binding affinity. No binding was observed for 5′-CMP and the remaining 5′-mononucleotides have the lowest affinity (5′-TMP > 5′-AMP > 5′-GMP) comparing with longest oligonucleotides used in this study. As expected the K_D values increase when nucleotide number increases. Indeed, the highest affinities are found for poly 30 series, namely $polyC_{30}$ to histamine and $polyA_{30}$ to agmatine surface. In general polyT and polyG series show lowest affinity with histamine, as well as, $polyT_3$, $polyT_{30}$, 5′-GMP and $polyG_6$ with agmatine (Table 1).

The order of K_D values for hetero-oligonucleotides binding to histamine and agmatine are similar and CCCTTT shows the highest affinity indicating that the presence of cytosine or adenosine increase the binding to the surfaces; while GGGTTT exhibited the lowest affinity, meaning that thymidine and guanosine together

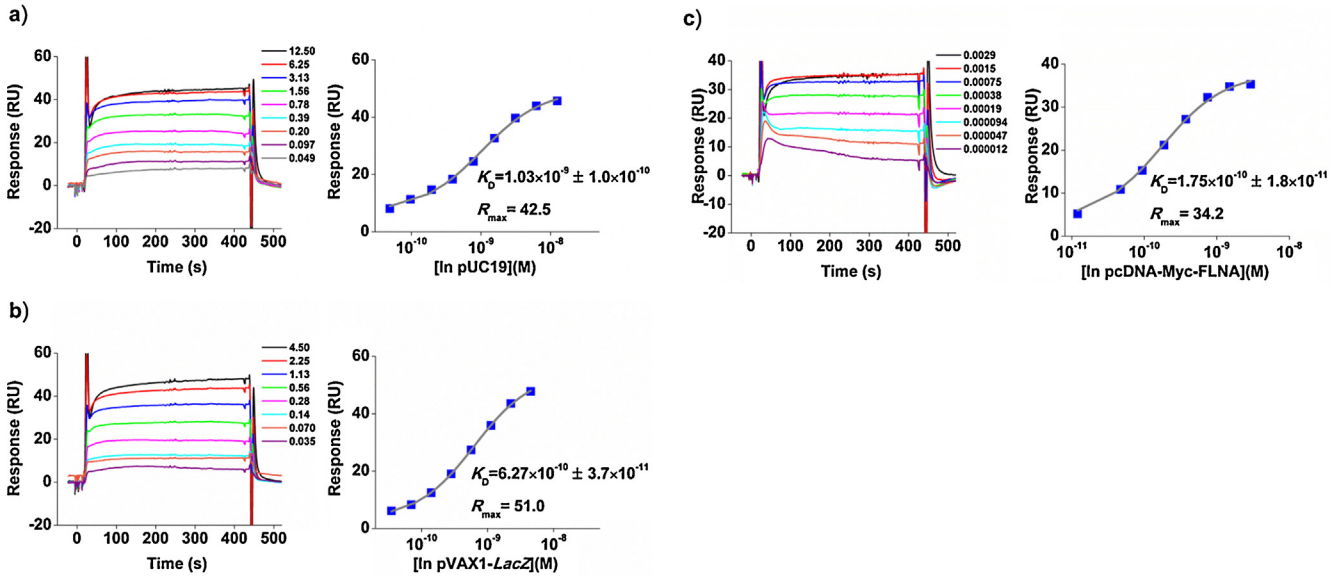

Fig. 5. Sensorgrams and equilibrium-binding analysis of immobilized histamine to linear isoform of (a) pUC19, (b) pVAX1-*LacZ* and (c) pcDNA3-myc-FLNa S2152A in 10 mM Tris–HCl pH 8.

decrease the binding strength to both surfaces. There are no significant differences in K_D values for the others sequences and the affinity is weaker ($K_D \approx 4 \times 10^{-4}$ M).

Previous studies performed by SPR-biosensor using L-arginine and L-histidine immobilized on surface showed also weaker affinity ($K_D > 10^{-4}$ M) [14,15]. In general polyT showed the highest affinity to arginine surface and $polyG_{15}$ the lowest affinity. However with L-histidine surface the highest binding affinity was found for $polyA_6$ follow by $polyG_6$ and the lowest with polyC.

This indicates that polyamines histamine and agmatine, without negative charge, have different binding preferences to the oligonucleotides.

By taking advantage of the multiple sites of agmatine and histamine available, the interaction was also examined to three isoforms of several plasmids, which were chosen due to their different size, base composition and structural conformation, such as it is represented in Fig. 4.

The sensorgrams and the binding curves of linear isoforms to histamine and agmatine are presented in Figs. 5 and 6, respectively. Plasmid pUC19 presents an equal distribution of 25% of each base, while sequences of pVAX1-*LacZ* and pcDNA3-myc-FLNa S2152A revealed a presence of approximately 30% guanine and cytosine and less for adenine and thymine (≈20%).

On contrary to the oligonucleotides, the overall affinity of plasmids to both surfaces was significantly stronger ($K_D > 10^{-7}$ M) and the identical RU values determined is due to the less concentration of pDNA samples (typically between 12.5 μM and 0.012 nM) needed to reach a plateau during the injection, while the concentrations of oligonucleotides needed to reach the plateau are higher, between 5.3 mM and 6.3 μM. There are significant differences in apparent affinity with the three plasmids isoforms. The affinity of plasmids isoforms is highest with histamine than with agmatine in the conditions used. The pVAX1-*LacZ* and pcDNA3-myc-FLNa S2152A showed the highest binding on both surfaces, while the pUC19 showed the lowest binding. These results suggest a linear tendency between plasmid size and binding.

In a general way, for any given plasmid size, the affinity is highest for the linear isoform with both surfaces followed by the oc and then the sc isoforms. For the 2.69-kbp plasmid, the K_D values for oc and linear isoforms has the same order of magnitude with agmatine and histamine, while with the 6.05-kbp and 14-kbp plasmids, there were differences in the affinity for these isoforms (see Table 1). Indeed the binding increase 5-fold for linear pcDNA3-myc-FLNa S2152A.

Similar to the binding behaviour of plasmids with different sizes, also the isoforms that present more expanded structural conformations revealed a higher affinity interaction with agmatine and histamine. Supercoiled pDNA isoform is the most compact conformation while oc and linear isoforms are more relaxed. In fact, the results suggest that the distention of these molecules provides more contact points to bind to the surfaces of derivative amino acids, since there is no presence of the carboxyl group in the agmatine and histamine, avoiding the repulsion by the phosphate groups of the nucleic acids and favouring the ionic interactions under the used conditions. Therefore, the higher affinity by the linear isoforms could be attributed to their relaxed form associated to the largest radius of gyration [16].

The results obtained with agmatine are opposite to those obtained with L-arginine in the same conditions [14]. Indeed, the strongest interaction in the L-arginine surface study was found for the sc form because of its conformation that increases the bases exposition degree [14]. The supercoiling phenomenon is responsible by the torsion in the double chain of the sc isoform, which results in a more compact structure with lower surface area and higher availability and exposure of nucleotide bases [17]. Thus, the low affinity of the sc isoforms observed for the three plasmids in the present work could be related with the high compaction degree that minimizes the contact points and interaction with histamine and agmatine ligands. Furthermore, the lower affinity of the scpVAX1-*LacZ* and pcDNA3-myc-FLNa S2152A isoforms in relation to the sc pUC19 isoform can be associated with the higher content of the guanosine (30%) in these two plasmids. As it was previously mentioned, the guanosine-based oligonucleotides presented a decreased binding strength to both surfaces.

In order to examine buffer composition and pH effect on the interaction behaviour of the different plasmid structures, four buffers (10 mM Tris–HCl with 1 M NaCl pH 8, 50 mM sodium citrate pH 5, 10 mM sodium acetate pH 5, 10 mM Tris–HCl pH 6) were used in the pVAX1-*LacZ* linear isoform interaction with agmatine and histamine. No binding response was detected for these distinct buffers, excepted for Tris 10 mM pH 6 with a binding increased ~3-fold for agmatine ($2.26 \times 10^{-10} \pm 2.1 \times 10^{-11}$) and slightly

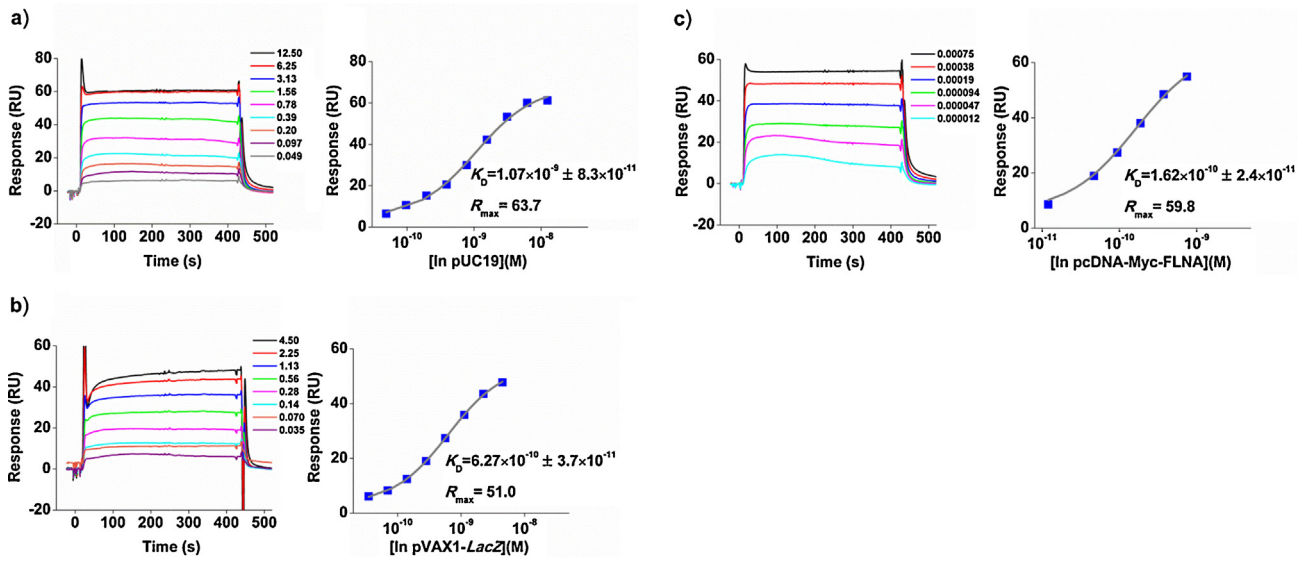

Fig. 6. Sensorgrams and equilibrium-binding analysis of immobilized agmatine to linear isoform of (a) pUC19, (b) pVAX1-*LacZ* and (c) pcDNA3-myc-FLNa S2152A in 10 mM Tris–HCl pH 8.

~1.2-fold for histamine ($5.07 \times 10^{-10} \pm 1.9 \times 10^{-11}$). This indicated that operating the ligands below pH 6 increased the affinity of linear isoform to both surfaces. The supplementation of the Tris buffer (pH 8) with 1 M of NaCl showed that the increase of ionic strength reduces the electrostatic attraction exerted by the surfaces [18].

Previous affinity chromatographic experiments using histamine immobilized to a monolithic support revealed that this multimodal ligand efficiently separates pDNA isoforms by manipulating the ionic strength in the mobile phase (ionic or hydrophobic conditions) and by changing the pH [12]. Our affinity data shows that Tris–HCl is an optimal buffer for interaction assays and distinct buffer environments such as sodium acetate, sodium phosphate or sodium citrate did not enhanced the binding to agmatine and histamine. We also verified that the interaction strength his dependent of pH since Tris–HCl below pH 6 allows effective linear plasmid binding to both surfaces. Knowing that the pK_a of agmatine and histamine is 9.07 and 7.05 respectively [12], the pH 6 in the buffer increases the effective charge of the surfaces (positive charge) mainly in the agmatine surface, resulting in the strengthening of electrostatic interactions with the plasmid isoform.

Overall, these results obtained with the biosensor provide the basis for the design of ligands that specifically target only one isoform, thereby increasing selectivity and improve efficient plasmid separation. It was also proved that under these conditions (ionic strength, pH and buffer composition) the electrostatic interactions are favoured between the amino positive groups of the agmatine and histamine and the negative phosphate groups of the different plasmids isoforms. Curiously, the predominant interactions of arginine ligands are ionic and hydrogen bonds with the more exposed bases, mainly with guanosine [19,20]. For the histidine ligands, hydrophobic interactions namely π–π staking interactions are the predominant forces, also preferentially promoted with the more available bases, such as guanosine [21]. However, the present work showed that the lack of the carboxyl group in derivative amino acids, agmatine and histamine induces a binding behaviour significantly different from the arginine and histidine amino acids.

This experimental data allowed us to get binding information to improve plasmid purification using histamine or agmatine monolith supports in affinity chromatography. The conditions tested by SPR-biosensor revealed that the ionic interaction could prevail. By this way and to separate pDNA isoforms is possible to use Tris–HCl 10 mM pH 8 to promote the binding and elution by increasing NaCl concentration [22].

4. Conclusions

Agmatine and histamine were immobilized to a carboxymethyl-dextran matrix and studied as affinity ligands towards oligonucleotides and plasmids isoforms of pUC19, pVAX1-*LacZ* and pcDNA3-myc-FLNa S2152A. The oligonucleotides were used as models toidentify the binding preferences to the ligands. Their overall affinity with both amino acid-derivatives was significantly weaker ($K_D > 10^{-4}$ M) and the maximum response was found for histamine. The SPR results indicated that an increase in the number of bases and backbone to 30 units leads to the highest affinity, and poly T and poly G have the lowest affinity to both agmatine and histamine. For the hetero-oligonucleotides the highest binding affinity was found for CCCTTT and the lowest for GGGTTT with both surfaces. This is in accordance with the binding data of the homo-oligonucleotides sequences. The overall affinity of the plasmids to the surfaces was higher ($K_D > 10^{-10}$ M).

The pcDNA3-myc-FLNa showed the highest binding to both surface, while the pUC19 showed the lowest binding. The highest affinity was found for linear isoform of the three plasmids ($K_D > 10^{-10}$ M). The Tris–HCl is the optimal running buffer for these interaction assays and working below pH 6 enhance linear plasmid binding to agmatine and histamine surfaces. No binding response was found by using high salt concentrations (NaCl) or other buffers composition (sodium citrate, sodium acetate), evidencing the predominance of ionic interactions under the used conditions.

Acknowledgements

Carla Cruz and Ângela Sousa acknowledge the post-doctoral grants from FCT (SFRH/BPD/46934/2008 and SFRH/BPD/79106/2011, respectively). This work was supported by FCT, the Portuguese Foundation for Science and Technology (PTDC/EBB-BIO/114320/2009, PTDC/QEQ-MED/1931/2012), PEst-C/SAU/UI0709/2011 COMPETE and FCOMP-01-0124-FEDER-041068–Ref[a]. EXPL/QEQ-MED/1068/2013.The authors also acknowledge to John Blenis for the pcDNA3-myc-FLNa S2152A Addgene plasmid.

Appendix A. Supplementary data

Supplementary data associated with this article can be found, in the online version, at http://dx.doi.org/10.1016/j.ijbiomac.2014.06.044.

References

[1] Y. StormoG.D. Zhao, Nat. Rev. Genet. 11 (2010) 751–760.
[2] Z. Xie, S. Hu, J. Qian, S. Blackshaw, H. Zhu, Cell. Mol. Life Sci. 68 (2011) 1657–1668.
[3] A.M.J.J. Bonvin, R. Boelens, R. Kaptein, Curr. Opin. Chem. Biol. 9 (2005) 501–508.
[4] V.J. LiCata, A.J. Wowor, Methods Cell Biol. 84 (2008) 243–262.
[5] A.R. Hieb, S. D'Arcy, M.A. Kramer, A.E. White, K. Luger, Nucl. Acids Res. 24 (2011) 1–13.
[6] A.G. Kozlov, T.M. Lohman, Methods Mol. Biol. 922 (2012) 37–54.
[7] F.A. Tanious, B. Nguyen, W.D. Wilson, Methods Cell Biol. 84 (2008) 53–77.
[8] R. Gamsjaeger, R. Kariawasam, L.H. Bang, C. Touma, C.D. Nguyen, J.M. Matthews, L. Cubeddu, J.P. Mackay, Anal. Biochem. 440 (2013) 178–185.
[9] A.J. Ruiz-Chica, A. Soriano, I. Tunon, F.M. Sanchez-Jimenez, E. Silla, F.J. Ramirez, ChemPhys 324 (2006) 579–590.
[10] J. Ruiz-Chica, M.A. Medina, F. Sanchez-Jimenez, F.J. Ramırez, J. Mol. Struct. 480–481 (1999) 455–458.
[11] Y. Li, M. Kobayashi, K. Furui, N. Soh, K. Nakano, T. Imato, Anal. Chim. Acta 576 (2006) 77–83.
[12] U. Cernigoj, U. Vidic, M. Baruta, A. Podgornik, M. Peterka, A. Strancar, J. Chromatogr. A 1281 (2013) 87–93.
[13] M.S. Woo, Y. Ohta, I. Rabinovitz, T.P. Stossel, J. Blenis, Mol. Cell. Biol. 24 (2004) 3025–3035.
[14] C. Cruz, A. Sousa, F. Sousa, J.A. Queiroz, Anal. Methods 5 (2013) 1682–1686.
[15] C. Cruz, D.S. Sandra, J.C. Eurico, J.A. Queiroz, Int. J. Biol. Macromol. 56 (2013) 175–180.
[16] D.R. Latulippe, A.L. Zydney, J. Chromatogr. A 1216 (2009) 6295–6302.
[17] F. Sousa, T. Matos, D.M.F. Prazeres, J.A. Queiroz, Anal. Biochem. 374 (2008) 432–434.
[18] C.M. Ongkudon, M.K. Danquah, J. Chromatogr. B 878 (2010) 2719–2725.
[19] F. Sousa, D.M.F. Prazeres, J.A. Queiroz, J. Gene Med. 11 (2009) 79–88.
[20] A. Soares, J.A. Queiroz, F. Sousa, A. Sousa, J. Chromatogr. A 1320 (2013) 72–79.
[21] A. Sousa, F. Sousa, D.M.F. Prazeres, J.A. Queiroz, Biomed. Chromatogr. 23 (2009) 745–753.
[22] A. Sousa, A.M. Almeida, U. Cernigoj, F. Sousa, J.A. Queiroz, J. Chromatogr. A (2014), http://dx.doi.org/10.1016/j.chroma.2014.06.003 (in press).